Journal of Structural Geology, Vol. 4, No. 1, pp. 197 to 213, 1982
Printed in Great Britain

0191-8141/82/020197-16 $03.00/0

Microstructure and geochemistry of plagioclase and microcline in naturally deformed granite

SIMON K. HANMER*

Department of Geology, Dalhousie University, Halifax, Nova Scotia, B3H 3J5, Canada

(*Received* 23 *December* 1980; *accepted in revised form* 23 *October* 1981)

Abstract—Naturally deformed feldspars from foliated granites in a shear zone in Newfoundland exhibit transitional brittle–ductile behaviour. Brittle failure is subordinate to dynamic recrystallization, microcracking, strain enhanced diffusion and reaction enhanced ductility during the deformation. Both plagioclase (An_{28}) and K-feldspar are transformed to albite with increasing strain. Interaction of metamorphic and structural processes at the grain scale is emphasised. This is illustrated with examples of quartz-filled veins (segregation bands) in plagioclase and recrystallized polycrystalline aggregates in plagioclase and K-feldspar. The role of microcracking in plagioclase and of pre-existing internal growth structures in the formation of initially coarse grained recrystallized aggregates from large single crystals is suggested.

INTRODUCTION

ROCKS of the earth's continental crust are predominantly composed of two mineral species: quartz and feldspar. The ductile behaviour of quartz is now well documented (e.g. Carter 1976), to such a degree that natural deformation-induced fabrics can be computer simulated (Lister & Paterson 1979). The same cannot be said of the feldspars. Plastic strain in plagioclase has only recently been recognized (Borg & Heard 1970, Carter 1971, 1976). Dislocation motion has been identified in plagioclase (Lally *et al.* 1972, Lorimer *et al.* 1974, White 1975, Marshall *et al.* 1976, Marshall & Wilson 1976, Marshall & McLaren 1977a, 1977b) and more recently in K-feldspar (Williame & Gandais 1977, Williame *et al.* 1979, Sacerdoti *et al.* 1980). Most of the work on feldspars concerns Transmission Electron Microscope (TEM) study of both naturally and artificially deformed single crystals and aggregates, although some optical microscopy studies have been published (e.g. Seifert 1965, Vernon 1975, Debat *et al.* 1978). The response of feldspars to stress under variable conditions of temperature, pressure and pH_2O in natural rock aggregates has been described for both natural (e.g. Sturt 1969, Eisbacher 1970, Debat *et al.* 1975, Wakefield 1977, Lister & Price 1978, Sylvester *et al.* 1978, Burg & Laurent 1978, Berthé *et al.* 1979a, Vidal *et al.* 1980) and artificial strains (e.g. Stesky 1977, Tullis & Yund 1977, 1980, Tullis *et al.* 1979).

Whereas the laboratory studies clearly indicate the existence of a brittle–ductile transition in the feldspars, which lies within the field of physico-chemical conditions typical of the continental crust, descriptions of feldspars in naturally deformed rocks abound with such terms as 'cataclasis, rupture, fractured, shattered, broken, comminuted, granulated and crushed'.

The object of the present contribution is to describe the optical microstructure of examples of naturally deformed plagioclase and K-feldspar showing transitional behaviour and to examine the chemical and mineralogical modifications which accompany the deformation at the grain scale.

(a) Some quartz veins in plagioclase, classically interpreted as brittle dilational structures, are shown to be ductile and non-dilational in origin.

(b) Some dynamically recrystallized aggregates of K-feldspar and plagioclase compare morphologically with published descriptions of dislocation associated recrystallization. Other aggregates do not. The contrast is attributed to the influence of microcracking and the pre-existing growth structure in the latter case.

The observations are discussed and briefly compared with published TEM work on similar microstructures.

In the following descriptions 'old' or 'host grains' refers to the feldspar megacrysts; 'subgrains' are regions of the old grain, misoriented by up to 10–15 degrees with respect to the old grain; 'new grains' are regions misoriented by more than 10–15 degrees to the old grain (Nicolas & Poirier, 1976, p. 170); 'aggregates' are polycrystalline aggregates derived by the recrystallization of single old grains; 'matrix' refers to the quartz and mica components of the rock.

GEOLOGICAL SETTING AND MACROSCOPIC STRUCTURE

Oriented specimens were collected from a suite of syntectonic diapiric granites, intruded into and deformed in a major Acadian shear zone in Northeastern Newfoundland, hereafter called the Northeast Newfoundland Shear Zone (N.N.S.Z. Fig. 1). The granites are coarse grained with large microcline (< 5 cm) and plagioclase (An ≃ 28; < 3 cm) megacrysts; set in a quartz–biotite matrix (Strong *et al.* 1974, Strong & Dickson 1978, Jayasinghe 1978). The structure of both the granites and country rock gneisses is attributable to

*Present address: Geology Department, Carleton University, Ottawa, Ontario, K1S 5B6, Canada.

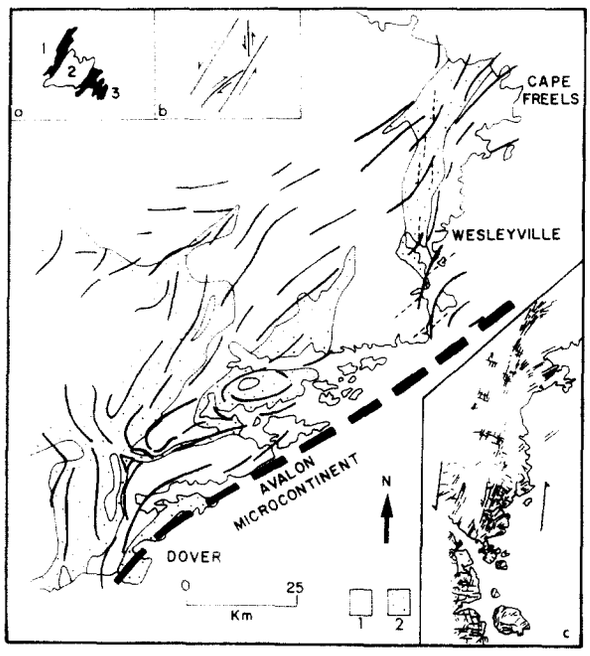

Fig. 1. Schematized geology of Northeast Newfoundland Shear Zone. Lithologies are (1) granites and (2) undifferentiated metamorphic country rocks. Continuous lines: foliation traces. Broken lines: crenulation cleavage ('C'' or shear band foliation) (only locally illustrated for clarity). Insets; a: location map with eastern continental margin of North America (1), Central Mobile Belt (2) and Avalon Micro-continent (3). b: Shear system with main sinistral N.N.S.Z., sinistral Cape Freels shear (Riedel 'R') and dextral Dover Fault (Riedel 'R''). c: Lineament map traced from air photos showing regional foliation and Cape Freels sinistral shear.

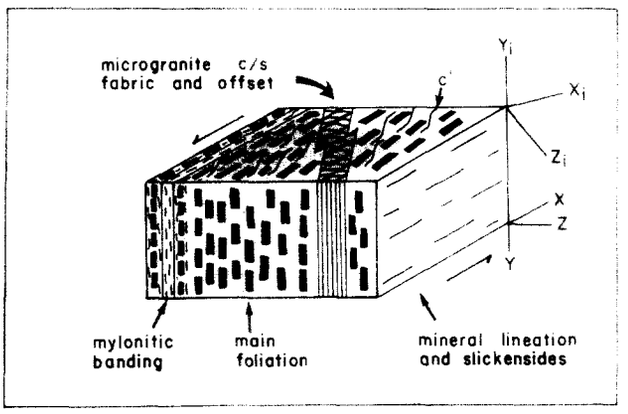

Fig. 2. Schematic illustration of mesoscopic strain criteria. Foliation of megacrystic granite passes into 'C' planes of late syntectonic microgranite intrusive sheet, and laterally grades into mylonite belts (left). Mineral lineation and/or slickensides (right) give shear direction. 'C' and 'S' planes within microgranite, vein-offsets and 'C'' or shear band foliation give shear sense and approximate orientations of finite (X, Y, Z) and instantaneous (X_i, Y_i, Z_i) strain ellipsoids (Ramsay & Graham 1970, Berthe *et al.* 1979a), see text.

interference between the local strain fields associated with the rising, expanding diapirs and the regional strain field generated by contemporaneous progressive sinistral movement across the 60 km wide ductile shear zone (Hanmer 1981a).

The shear zone separates the Avalon microcontinent to the east from the Central Mobile Belt and the eastern continental margin of North America to the west (Williams 1979). Recent palaeomagnetic models for the Upper Palaeozoic (e.g. Morris 1976, Kent & Opdyke 1978, Van der Voo *et al.* 1979) predict up to 2000 km of sinistral offset between Avalonia and Cratonic North America, part of which has been accommodated by the N.N.S.Z. (Hanmer 1980, 1981a). From its size and geological context, the N.N.S.Z. may represent a deeply eroded fossil analogue of modern day large scale transcurrent shear zones.

Internally the granites carry a variably developed upright, planar foliation marked by quartz leaves and feldspar megacrysts; the latter often carry macroscopic quartz veins oriented at 45 to 90 degrees to a horizontal mineral lineation developed on the foliation. From its relationship to the injection of pegmatite, aplite and microgranite sheets (Hanmer 1981a), the foliation formed while the granites were still hot at approximately 500–600°C. Deformation apparently continued during cooling. The presence of kyanite in the country rocks (Blackwood 1977, Jayasinghe 1978) suggests intermediate confining pressures of about 5 kb. At low to moderate bulk strains (moderately foliated and lineated specimens), short planar shears, similar to the 'C' planes of Berthé *et al.* (1979a), are locally developed at an angle of 45 degrees or less to the foliation (Fig. 2). However, they are only clearly visible on cut and varnished faces. In the field the foliation grades laterally through all stages to ultramylonite.

The foliation is crossed by a moderately developed crenulation cleavage, composed of centrimetrically spaced, discrete shears (Fig. 1 and 2) identical in style and orientation to the 'C'' planes of Berthé *et al.* (1979b) or shear band foliation of White *et al.* (1980). The shears form two spatially separated and differentially oriented families, each of which is a small scale equivalent of one of the two mapping scale shear zones which deform the main N.N.S.Z. foliation (Fig. 1). From the sense and orientation of these small scale shears and mapping scale shear zones, with respect to the N.N.S.Z., they are analogous to Riedel (sinistral 'R' and dextral 'R'') shears (Hanmer 1981a).

In the field, the direction and sense of shear at the outcrop scale are given by (a) the mineral elongation lineation, (b) vein boundary offsets, (c) 'C' and 'S' planes (Berthé *et al.* 1979a) in syntectonic microgranite sheets and (d) 'C'' or shear band foliation (Fig. 2).

Oversize (10 × 15 cm) thin sections were cut perpendicular to the macroscopic foliation and parallel to the mineral lineation. All were stained for K-feldspar (Deer *et al.* 1966, p. 311), except for the microprobe preparations. All optical microscopy was performed on a flat stage, so that all angles measured are minimum apparent values. The samples, ranging from very mildly foliated granites to mylonites, were taken from different outcrops within the N.N.S.Z.

PLAGIOCLASE MICROSTRUCTURE

Segregation bands

En-echelon quartz filled veins, oriented at 45 degrees to

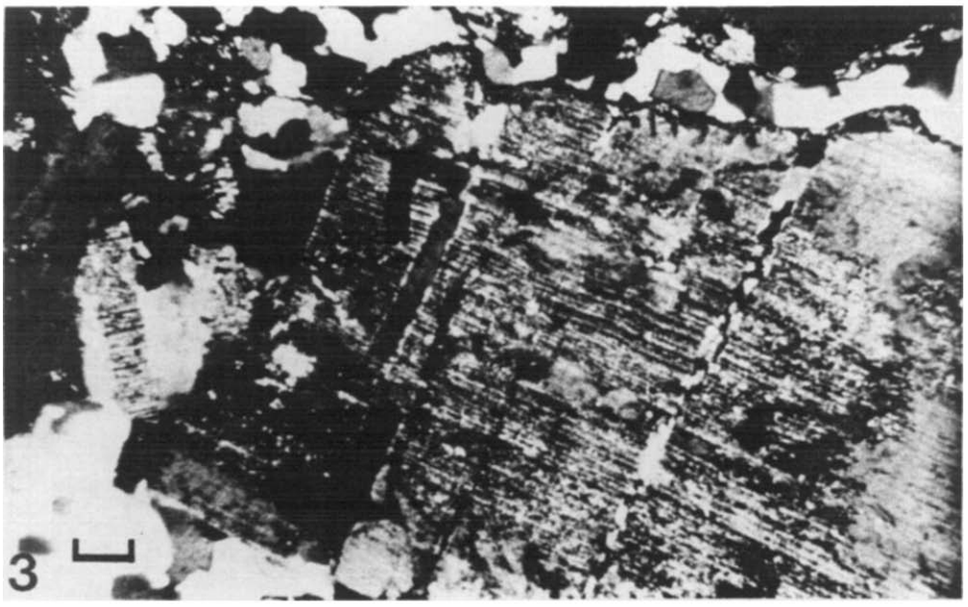

Fig. 3. Mature segregation bands, either intragranular (centre) or transgranular (centre right). A quartz core, either monocrystalline or polycrystalline is bounded by thin sodic plagioclase selvedges. Scale 100 μm.

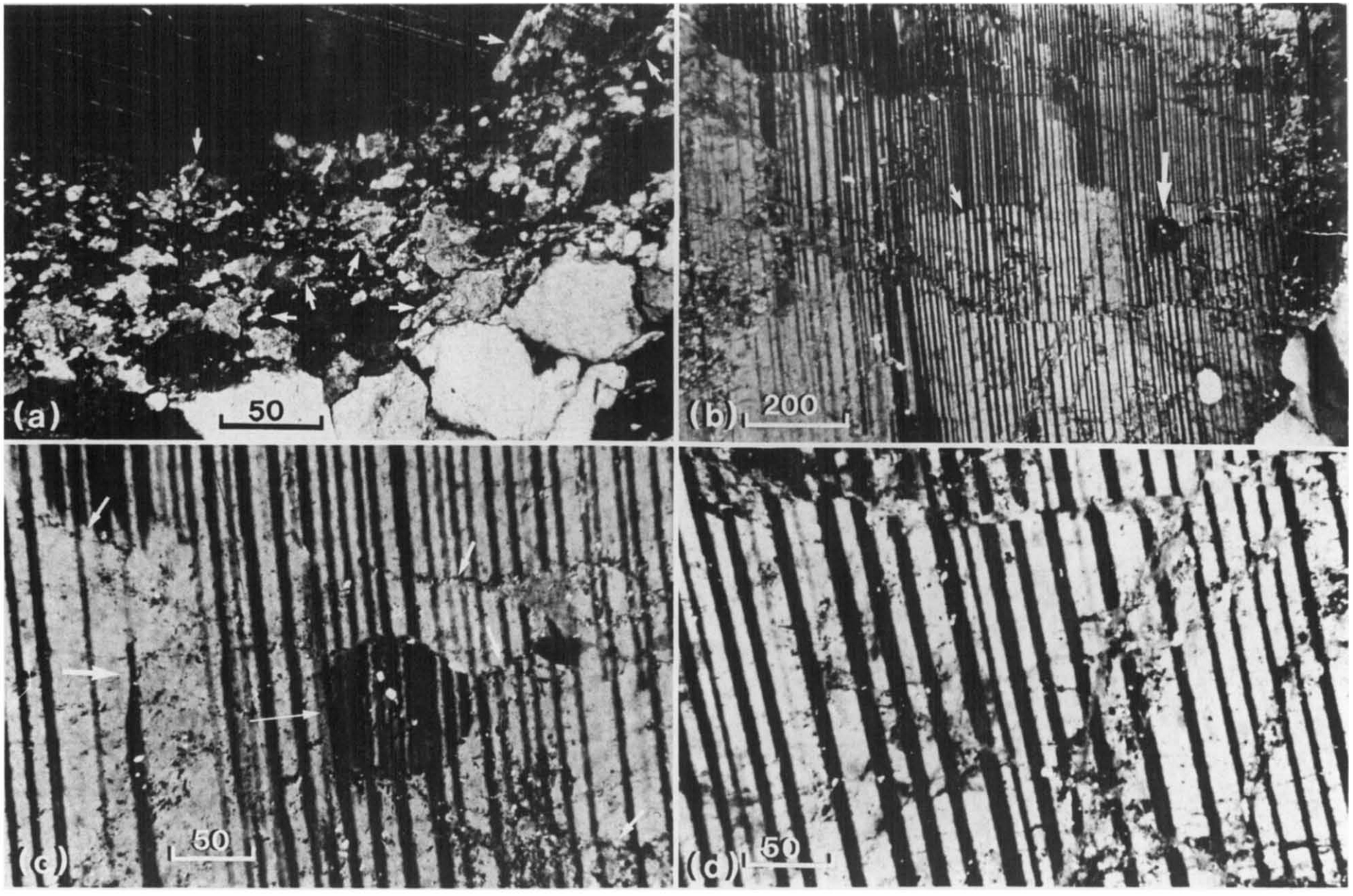

Fig. 5. (a) Plagioclase core (top), recrystallized type IP mantle aggregate of sodic plagioclase and interstitial biotite (arrows), quartz matrix (bottom right). (b) Homogeneous distribution of large type IIP subgrains mutually misoriented ($\approx 2^\circ$) across boundaries sub-perpendicular to (010) (small arrow). Marked rotation of small subgrain (large arrow). (c) Detail of small subgrain in b. Distinct misorientation by rotation. Left-hand boundary not yet discrete (thin arrow). Note wedge-like termination of mechanical twin in host (thick arrow). Note sericite decorated anastomosing zones at high angle to (010), bounding mildly misoriented subgrains (small arrows). (d) Detail of sericite decorated subgrain boundaries. Note absence of twinning within and offset across the zones. Compare with descriptions of stress-corrosion microcracks (Kerrich *et al.* 1980). Scale bars in microns

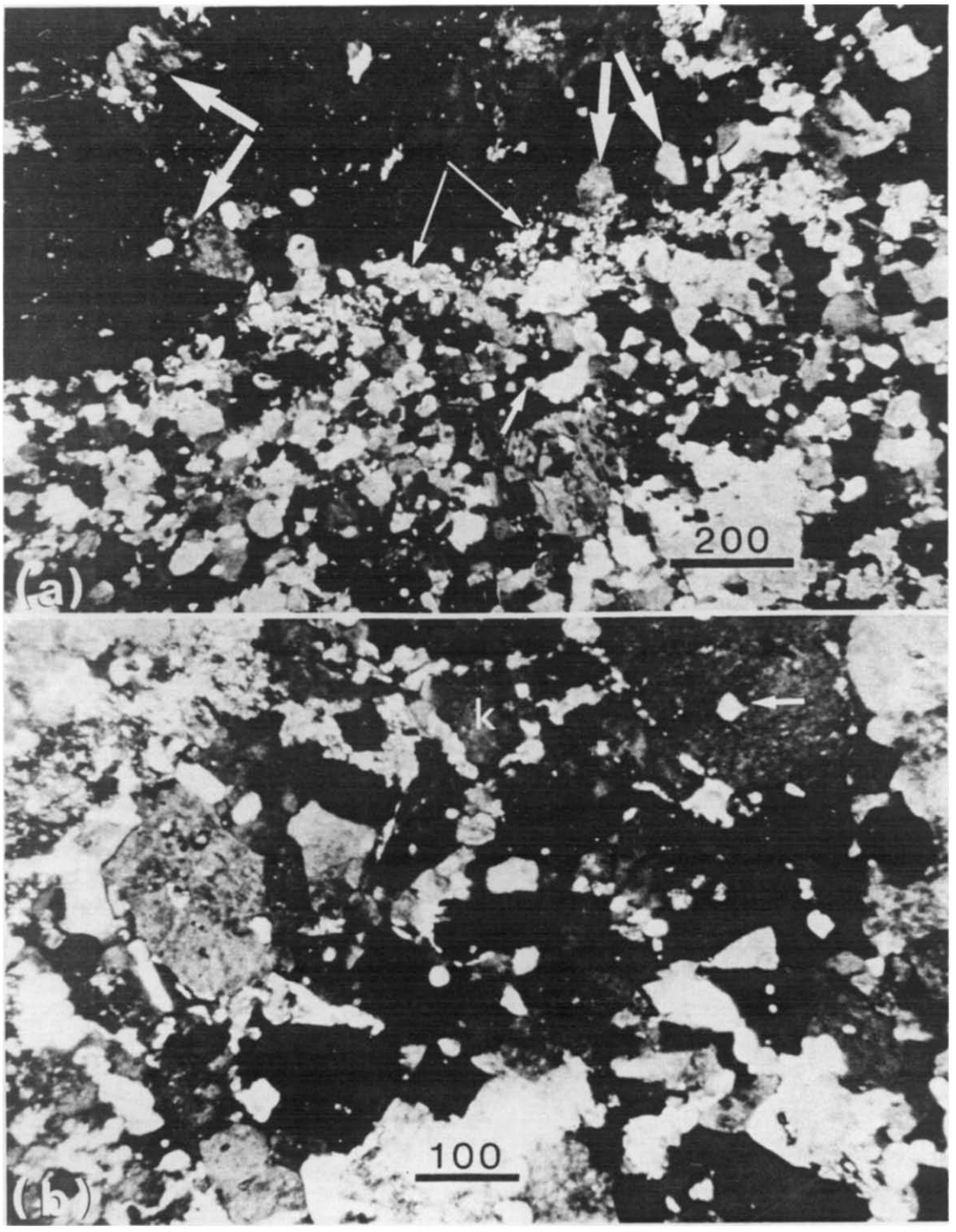

Fig. 6. (a) Matrix (bottom right), type IM K-feldspar/sodic plagioclase mantle aggregate with abundant interstitial quartz drops (small arrows), sericitized inner mantle plagioclase new grains (long arrows) and host K-feldspar core (top left). K-feldspar new grains in outer core (thick arrows). (b) Misoriented, polygonal small K-feldspar new grains (dark e.g. K) with interstitial sodic plagioclase new grains at boundaries and triple points in a type IIM aggregate. Some intragranular plagioclase (arrow). Scale bars in microns.

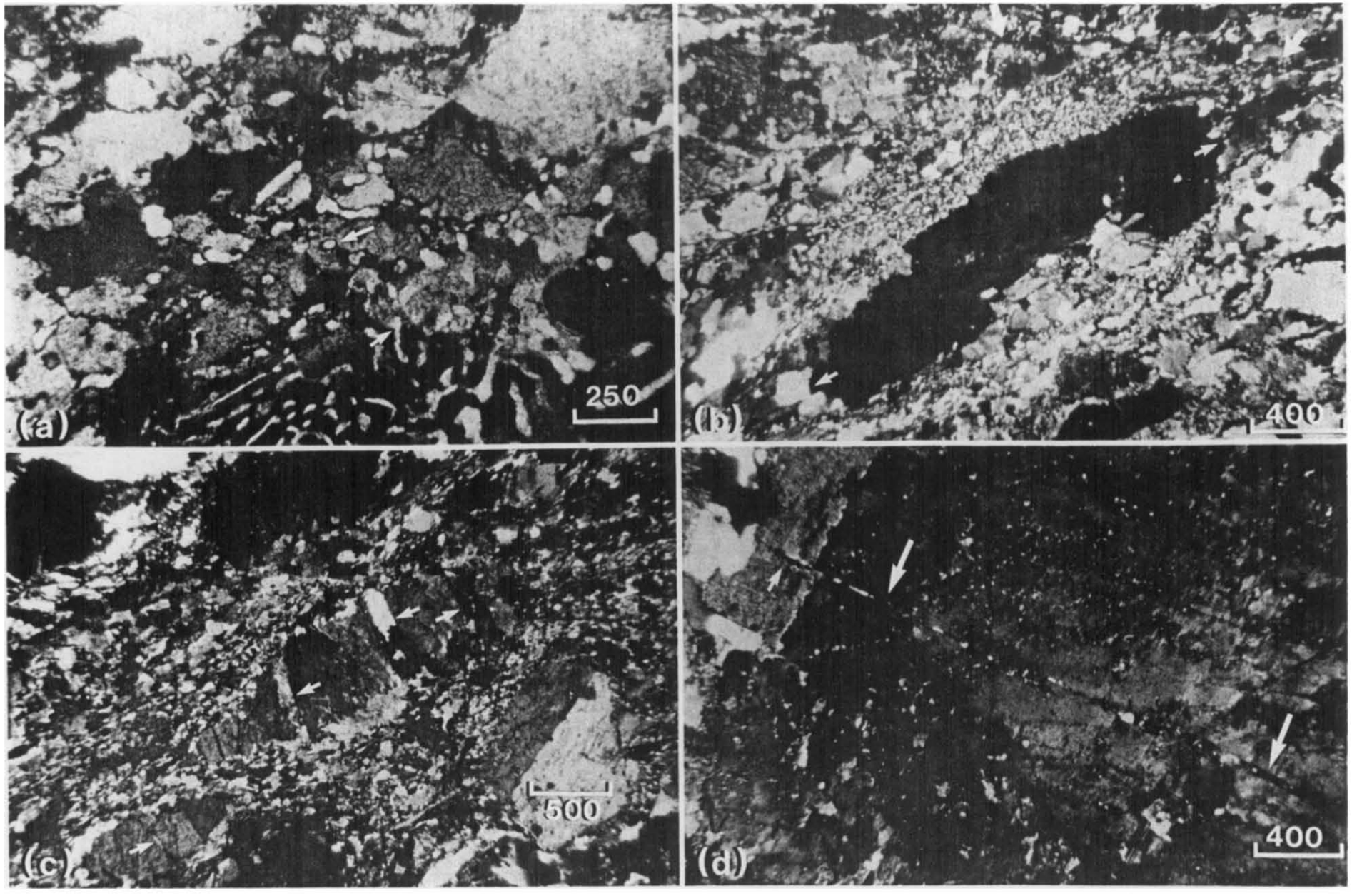

Fig. 7. (a) Detail of plagioclase new grains, quartz drops (large arrow) in type IM mantle aggregates. Myrmekite vermicules of quartz (bottom) develop across plagioclase new grain boundaries (small arrow), see Fig. 8(j). (b) Microcline core with fine grained sodic plagioclase mantle especially well developed on upper left side. Larger K-feldspar new grains at ends (small arrows). Shear plane (E–W) just visible in top field (large arrows), see text. (c) As b; note the intragranular veins within the core (arrows) stop abruptly at the core-mantle boundary. The fine grained sodic plagioclase mantle extends NE–SW to the edges of the photo. (d) Kink band traversing K-feldspar (large arrows) decorated by single chain of K-feldspar and sodic plagioclase new grains (light). Passes in continuity into minor albite selvedged quartz-filled segregation band in adjacent plagioclase (small arrow). Scale bar in microns.

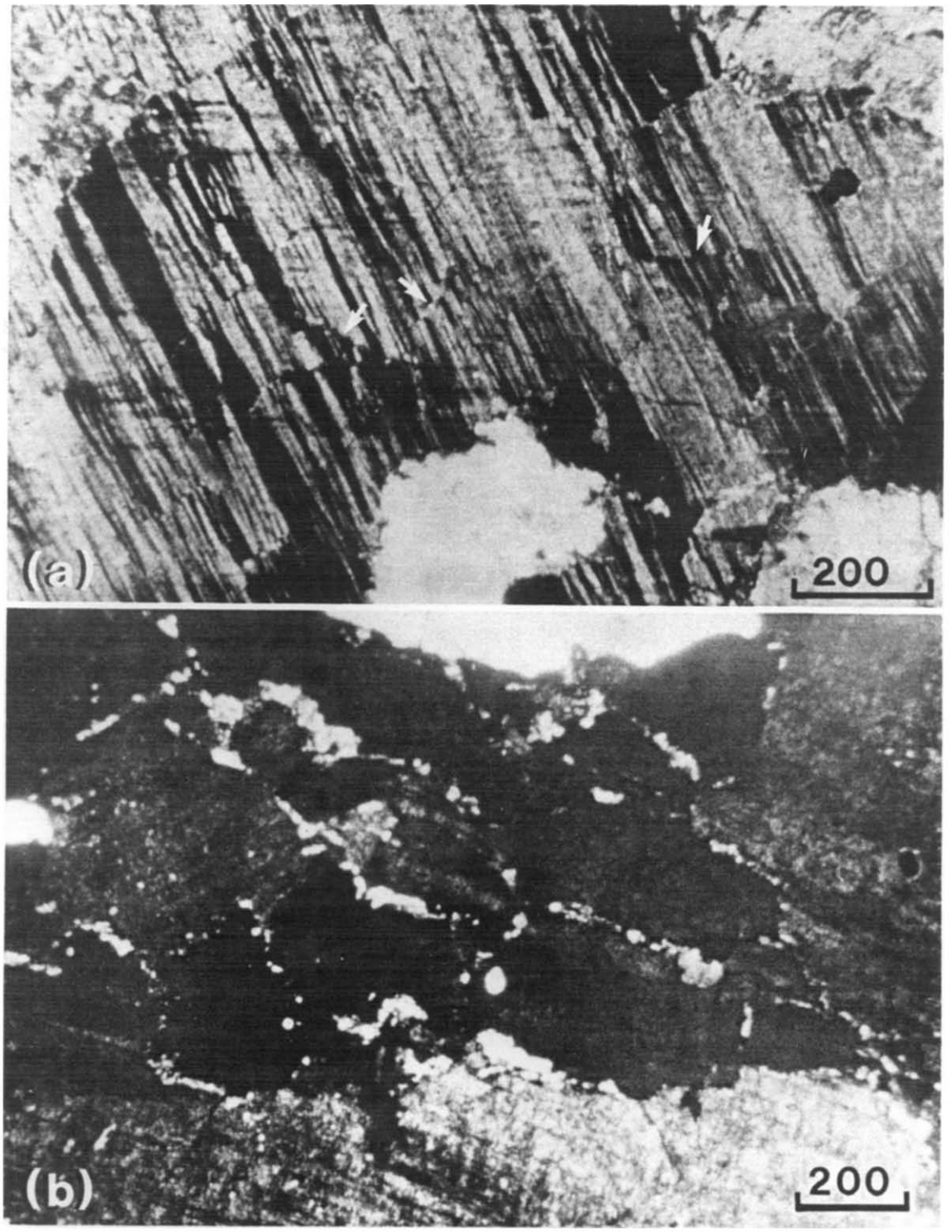

Fig. 9. (a) Initation of large lozenge-shape domains in microcline type IM substructure. Dominant microcline twins (NW–SE), subordinate microcline twins (E–W) and conjugate shears enclosing the domains (arrows). Note dominant microcline twins bisect obtuse angle between shears. One of the shears (right arrow) parallel to subordinate twins. (b) Misoriented coarse, irregular, K-feldspar domains (dark) in type IIM aggregate adjacent to K-feldspar host (bottom). Note single chains of small sodic plagioclase new grains (light) decorating K-feldspar domain boundaries.

the shear plane, are commonly recorded in deformed feldspar as 'tension cracks or gashes' (e.g. Debat *et al.* 1978). They are classically interpreted as brittle dilational structures (e.g. Beach 1975, Knipe & White 1979). Similar intragranular veins examined in this study are described in detail elsewhere and are called segregation bands (Hanmer 1981b).

The simplest segregation bands do not contain quartz. They comprise 25–10 μm wide bands of sodic plagioclase within the more calcic host grain and lie at a high angle to the host (010) lattice plane. The segregation band is 'clean' compared to the commonly inclusion and sericite dusted host plagioclase. However, the segregation band boundaries are often associated with anomalously high concentrations of sericite. Segregation bands are divided into three arbitrary types: Type (1); the host grain twin lamellae end at the segregation band boundaries and the segregation band is twin-free. Type (2); host grain twin lamellae pass in structural continuity across the segregation band. Within the segregation band, the twins are deflected through 10–30 degrees and the segregation band is a kink band with rounded hinges. Type (3); host twin lamellae pass into the segregation band, but are abruptly offset across a discrete discontinuity. The discontinuity lies in the plane of the segregation band and divides it symmetrically into two portions. Segregation bands of types (2) and (3) are parallel to, and show the same synthetic sense of shear as, the specimen scale shear band foliation. Furthermore, all three types of segregation band lie parallel to and, in the case of types (2) and (3), show the same sense of offset as non-albitized intragranular kink bands in the same specimen.

Quartz beads, 10 μm across, occur in single file along the centres of more complex segregation bands, irrespective of band type. All intermediate morphologies between isolated beads and a continuous, often monocrystalline, quartz core, bounded symmetrically by narrow sodic plagioclase selvedges (Fig. 3), may be seen in a single specimen. The preservation of type (2) and type (3) microstructural features, in the sodic plagioclase bridges between the quartz beads, suggests a developmental sequence from incipient sodic plagioclase bands through to mature segregation bands with continuous quartz cores. In more complex examples, other phases may accompany, or entirely occupy the place of, the quartz core: e.g. epidote, clinozoisite, muscovite, chlorite, magilmenite (Fig. 4).

Deformation twins

The majority of twins in the plagioclase obey the albite twin law. However the association with pericline-law twins, even in the most mildly deformed samples, suggests that many of the twins are mechanical (Marshall & Wilson 1976). The albite twin morphology (Fig. 5b) corresponds to that of deformation twins described by White (1975). Pericline twins are not abundant. Rarely homogeneously distributed through the grain, they tend to be concentrated in discrete subequant zones within which, if sufficiently closely spaced, they obliterate the albite twins. White (1975) describes a similar configuration observed at the sub-microscopic scale.

Recrystallization

Recrystallization in the plagioclase results in two types of new grain aggregate, types IP and IIP, both of which are apparently, within the limits of microscopic observation, associated with the rotation of substructural elements.

Type IP new grain aggregates tend to predominate at relatively high bulk strains (i.e. in well foliated rocks). The new grains are located adjacent to the host grain boundaries, especially those at a high angle to the maximum instantaneous shortening direction (inferred from the direction and sense of shear), and within zones of localized high intragranular strains such as isolated kink bands or shears. The resultant microstructure is therefore a predominantly core and mantle structure (White 1976).

At lower bulk strains, the new grains are confined to the marginal zones of the host grains at triple point contacts. At higher bulk strains the host grain margins are partial mantles, 50–100 μm wide, composed of 5–40 μm new grains (Fig. 5a). Such new grain aggregates may spread along the matrix foliation away from the host grain as asymmetrical tails. Within the host grains, new grains occur in narrow (up to 500 μm) kink bands. The new grains are associated with comparable size subgrains, which are slightly misoriented with respect to the host grain. Furthermore, both the new grains and subgrains exhibit undulose extinction. Both mantle aggregates and aggregates in kink bands and shears are frequently associated with interstitial biotite or chlorite. The size of the plagioclase new grains varies with the size of the

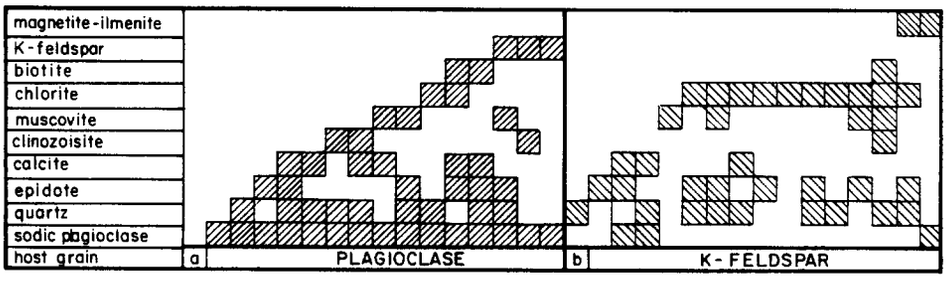

Fig. 4. Mineral assemblages observed within segregation bands in (a) plagioclase and (b) K-feldspar.

phyllosilicates (20–100 μm long), although the latter have a consistent 4:1 aspect ratio (Fig. 5a).

The type IIP new grain aggregates differ from type IP by (a) a coarser grain size (100–500 μm cf. 5–40 μm); (b) an intragranular distribution of new grains independent of host grain boundaries and isolated kink bands and shears; (c) a general lack of accessory interstitial biotite and (d) predominance at relatively low bulk strains.

At relatively low bulk strains (i.e. in poorly foliated rocks), a domainal substructure is visible in some plagioclase old grains sectioned at high angle to (010). Observed as a patchwork extinction pattern, the domains are homogeneously or randomly distributed within the host grain and are misoriented with respect to the host lattice (Fig. 5b). These domains are here called subgrains, though use of this term will be discussed below.

The subgrains are sub-rectangular, equant and bounded by (010) and (001) planes. They are large, generally 100–500 μm across, though occasionally smaller subgrains do occur (30–50 μm). Initial misorientation of the subgrains with respect to the host grain is about 2°. Albite twins are apparently continuous across non-discrete subgrain walls. Twin density within the subgrains may be greater or less than that of the host grain (Fig. 5b) and in some cases albite twinning is absent and has presumably been destroyed. Such twinless subgrains are occasionally associated with rare clinozoisite grains and are 'clean' relative to the impurity dusted host grains. Where the albite twins within the subgrains are visibly discontinuous and misoriented (2–5°) with respect to those of the host grain, the subgrain boundary is discrete. Misorientation occurs by progressive rotation as evidenced by examples where albite twins on one side of the rotated subgrain are still continuous with those of the host grain (Fig. 5c). Progressive misorientation of the subgrains, up to an observed maximum of 25° with respect to the host grains, results in the formation of coarse new grains.

The subgrain boundaries may be discrete discontinuities or zones of feldspar 1–5 μm wide, in which the albite twinning has been destroyed. The zones may be simple or compound and anastomosing (Figs. 5c & d) and small (< 5 μm) phyllosilicate grains (e.g. sericite) are distinctly concentrated along them. In these respects, therefore, the boundaries are similar to the type (1) segregation bands described above.

The discrete domains of dense pericline twins constitute a variety of IIP subgrain, bounded by the albite twins of the host grain and the pericline twins of the subgrain itself. In yet another variation, subgrains with internal albite twins may be bounded by planar pericline twins of the host grain. The misorientation of these subgrains has not been observed to exceed a few degrees.

K-FELDSPAR MICROSTRUCTURE

The K-feldspar megacrysts contain en-echelon quartz veins. While many are clearly brittle dilational structures, others are more ambiguous and will not be further considered here.

Recrystallization

K-feldspar presents a sequence of structures passing progressively from large subgrains of host composition, via smaller new grains of K-feldspar to fine grained sodic plagioclase new grains. As in plagioclase, two types of new grain aggregate are recognized: type IM and type IIM. Type IM aggregates are associated with core and mantle structure, whereas in type IIM aggregates the interior of the old grain is reduced either to a mortar structure or to a homogeneous polycrystalline aggregate.

In type IM aggregates, the first indication of recrystallization is the formation of 50–150 μm equidimensional subgrains and new grains of host composition. This is initially restricted to those host grain boundaries making a large angle to the instantaneous shortening direction. With increasing strain, the zone of marginal recrystallization broadens and extends all around the boundary of the host grain. Sodic plagioclase new grains (10–40 μm), initially sited at K-feldspar new grain boundaries and triple points, progressively replace K-feldspar grains and produce a plagioclase/K-feldspar new grain mantle aggregate (Fig. 6a). The replacement mechanism is however, not well preserved in these specimens since although the K-feldspar new grains show undulose extinction, no subgrains were noted within them (Fig. 6b). Small (10 μm), rounded drop-like quartz grains are evenly dispersed through the aggregate and occur at plagioclase grain boundaries and triple point contacts. The quartz drops most commonly occur where the plagioclase new grains are 40 μm or greater in diameter. Identical quartz drops occur as inclusions within the larger (100 μm) plagioclase new grains and may be indicative of grain boundary migration (Fig. 7a). Mechanical kinking, bend-

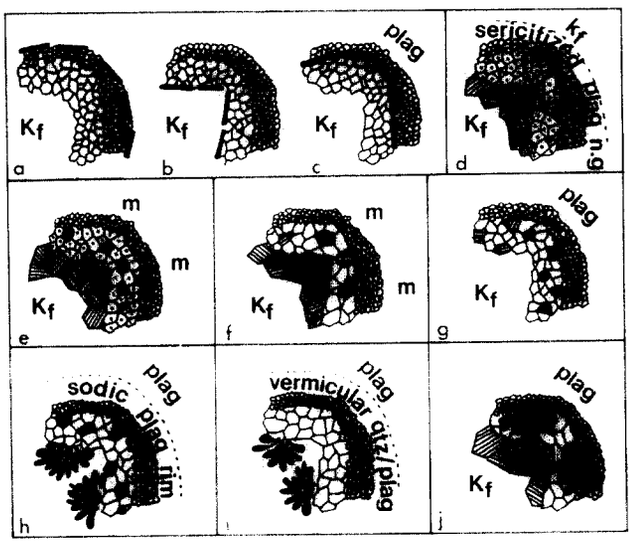

Fig. 8. Diagrammatic representation of observed varieties of core and mantle structure developed on K-feldspar. Cross hatching: K-feldspar new grains of the outer core. Single dots: sericitized sodic plagioclase. Blank: clean sodic plagioclase. 'Feather Dusters': myrmekitic quartz vermicules. Heavy black lines: biotite. M: matrix. N.G.: new grains. Other labels: adjacent porphyroblasts, with or without rims and mantles. In a, b and c, the position of biotite films indicates that the mantle aggregates are derived from the Kf core, sources other than the apparent core and from both the Kf core and adjacent plagioclase, respectively.

ing, subgrains and segregation bands may be present in the coarser plagioclase grains of the mantle aggregates.

The mantles may be homogeneous in mineral composition and grain size. More commonly they exhibit both grain size and compositional gradients (Fig. 8). From Figs. 7(a) and 8 several observations are made:

(1) In the absence of intervening phyllosilicate films, careful observation is required to assess the potential contribution of type IP mantles on adjacent plagioclase porphyroclasts to the type IM mantle structure (Figs. 8a–c).

(2) Sodic plagioclase new grains are preferentially sericitized adjacent to the K-feldspar core (Figs. 8d & e), which itself may contain sericitized perthite, plagioclase inclusions and new grains. This may suggest an original zonation of the mantle aggregate with respect to plagioclase composition.

(3) The predominantly sodic plagioclase mantle aggregate contains variable proportions of misoriented K-feldspar new grains (Figs. 8e–h). Their proportion diminishes from the outer core towards the outer mantle and generally accompanies an overall grain size decrease down to 10 μm. Note that inverse grain size gradients are also observed in wholly plagioclase mantle aggregates in these samples and probably reflect post-mantle grain growth.

(4) The coarser inner mantle plagioclase ($\approx 40\,\mu$m) is associated with quartz drops (10 μm) which are absent in the finer grained outer mantle (Fig. 7a).

(5) Myrmekite commonly occurs along the inner boundary of the new grain aggregates (Figs. 8h & i) i.e. the myrmekite forms within the old K-feldspar grain rather than at its contact with adjacent plagioclase porphyroclasts. Combined with the undeformed state of the delicate myrmekite structures, this suggests that the myrmekite post-dates the formation of the plagioclase mantles.

At higher strains, the width of the mantles increases, the relic K-feldspar new grains are eliminated in the aggregate and the grain size becomes uniform (10–25 μm, Fig. 7b). As in the case of type IP new grain aggregates in plagioclase, euhedral interstitial biotite grains are commonly disseminated through the type IM mantle aggregate. The K-feldspar cores may contain quartz filled veins of similar width to those observed in grains devoid of mantle aggregates at low bulk strains (Fig. 7c), which terminate abruptly against the inner mantle boundary.

At low bulk strains, small (15–25 μm) new grains of K-feldspar form along sporadic, isolated, very narrow, straight kink bands in the old grains. The new grains lie in single file along the kink. The K-feldspar new grains may be replaced by sericitized plagioclase new grains without change in the grain size. The kinks are structurally related to the segregation bands in the plagioclase feldspars, as indicated by an example of the one passing directly into the other at a K-feldspar/plagioclase old grain boundary (Fig. 7d).

The distinction made here between aggregates of types IM and IIM is based upon similar structural criteria to those which distinguish types IP and IIP. In type IIM aggregates, at low bulk strains, the host K-feldspar grain is divided throughout its volume into a coarse domainal substructure. In contrast to type IM aggregates, the distribution and development of the type IIM substructure is independent of host grain boundaries and isolated intragranular kink bands or shears. Two morphologically distinct type IIM domainal substructures may occur.

The first domainal substructure comprises equant to lozenge-shaped monocrystalline domains (200 μm long) bounded by straight, discrete discontinuities (Fig. 9a). The discontinuities forming the domain boundaries have the geometry of conjugate shears and are morphologically similar to structures described by Debat *et al.* (1978, fig. 7b) and to the deformation lamellae of Williame *et al.* (1979, fig. 13b). They are strongly crystallographically controlled as shown by their relationship to microcline twin planes: (a) the obtuse angle between the conjugate discontinuities is frequently bisected by the dominant set of twin planes and (b) one set of shears may lie parallel to the subordinate set of twin planes (Fig. 9a). The discontinuities are too thin to be resolved optically in any detail. However, they are often decorated by single-file chains of 15–25 μm sericitized plagioclase new grains. In the absence of new grains, sets of plumose "half-gashes" (Debat *et al.* 1978) of albite decorate the shears.

The second domainal substructure comprises generally equant, irregular monocrystalline domains, 600 μm to 2 mm across and optically misoriented to varying degrees with respect to the host grain (Fig. 9b). Undulose extinction is common. The domain boundaries are frequently decorated by smaller (50–100 μm) K-feldspar subgrains and new grains which themselves commonly show undulose extinction. The K-feldspar new grain aggregates may consume the domain boundaries. Alternatively, a subgrain in subgrain (*s.l.*) structure develops (e.g. White 1973) whereby the domains of the initial coarse substructure are reduced internally to clusters of irregular shaped, medium size (50–150 μm) K-feldspar subgrains and new grains.

The degree of internal recrystallization may obliterate the initial domain pattern. The original host grain is reduced to a largely recrystallized aggregate or mortar structure comprised of larger relic fragments of K-feldspar, surrounded by irregular to polygonal K-feldspar new grains, which range in size from 50 to 150 μm. Small (10–40 μm) plagioclase new grains form along the boundaries and at the triple point contacts of the K-feldspar new grains. Although the K-feldspar new grains and subgrains show undulose extinction, suitably small subgrains are not seen to accompany this replacement. Identical plagioclase new grains may form directly at the domain boundaries (Fig. 9b). Further evolution of the mortar structure is analogous to that of the type IM mantle aggregates, where the K-feldspar new grains are themselves ultimately replaced by the fine grained plagioclase new grains.

Where internal recrystallization involves the entire host grain, the shape of the resultant K-feldspar or K-feldspar/plagioclase aggregate changes drastically. Smaller, coherent aggregates form elliptical bodies aligned parallel to the instantaneous strain ellipsoid (cf. Talbot

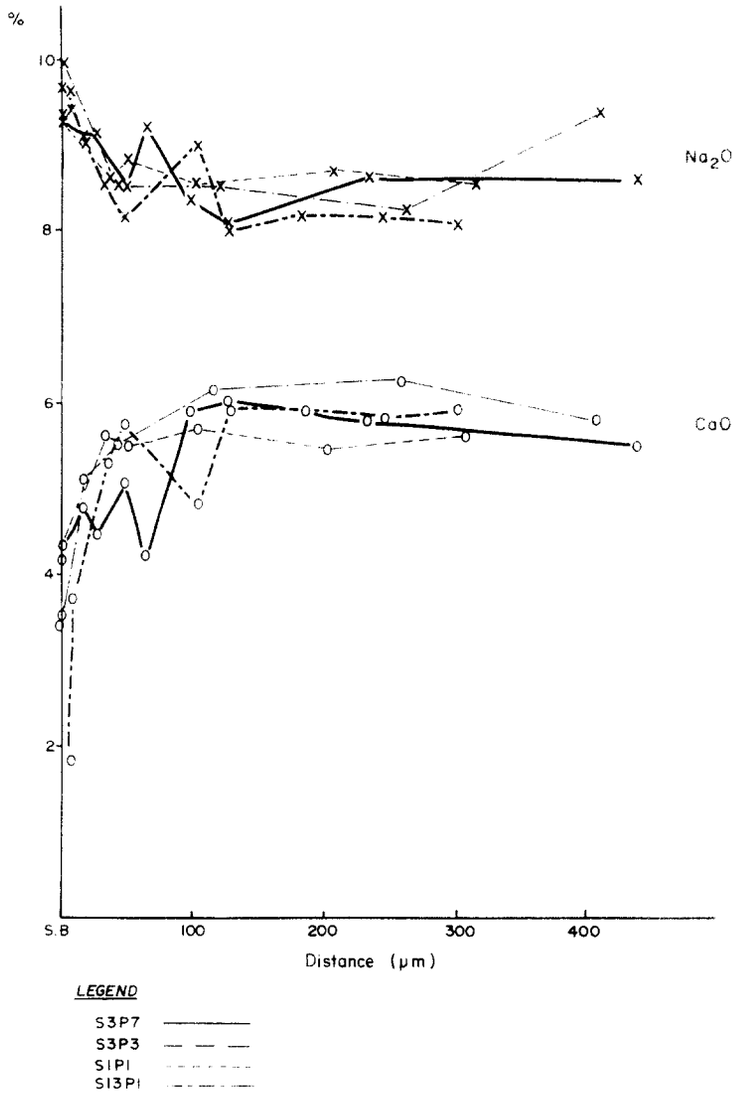

Fig. 10. Na_2O and CaO concentration with distance from segregation band boundaries (S.B.) in plagioclase.

1979). Larger aggregates form elongate thin bands, strung out, with or without boudinage, at angles of 0–45 degrees to the shear plane.

GEOCHEMISTRY

Chemical analysis of the feldspars has been undertaken using the Cambridge MKV microprobe (Ortee energy dispersive system) at Dalhousie University. The results are presented graphically.

Marked concentration gradients of Na_2O and CaO occur adjacent to the segregation bands in plagioclase and extend over distances of 100–200 μm from the band boundaries into the host grain (Figs. 10 and 11). The concentration gradients suggest that mass transfer by diffusion plays an active role in the transformation of calcic to sodium plagioclase in the segregation bands and indicate a maximum diffusion distance for Ca^{2+} and Na^{2+}. The range of compositions of plagioclase subgrains and new grains from type IP aggregates and of old plagioclase grains adjacent to the segregation bands is represented in Fig. 12.

Both old K-feldspars megacrysts and new grains from type IM aggregates show high K/Na + K ratios. The compositional range of the parent grains is reflected in the new grain compositions at low bulk strains (Fig. 13). However, the old grains at high bulk strains clearly tend towards a more limited compositional variation and slightly higher Si/Al ratios than the low bulk strain samples.

Data for centre to edge traverses across the cores of core-and-mantle structures in K-feldspars is inconsistent. Very mild depletion in K_2O at the core edge is apparently associated with a plagioclase mantle, whilst weak depletion at intermediate radii within the core is accompanied by K-feldspar/plagioclase mantles. Migration of K from intermediate radii towards the core edge may be related to the stability and persistence of K-feldspar new grains in the mantle.

Comparison of Figs. 12 and 14 suggests that plagioclase new grains in type IM aggregates are more

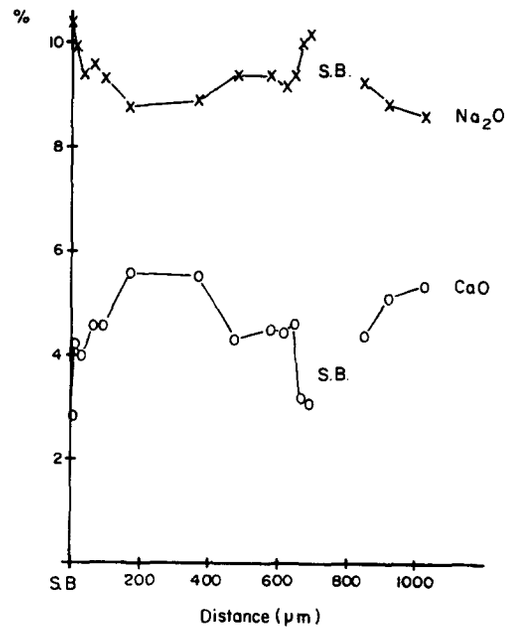

Fig. 11. Na_2O and CaO concentration with distance from two adjacent segregation bands (S.B.) boundaries in plagioclase.

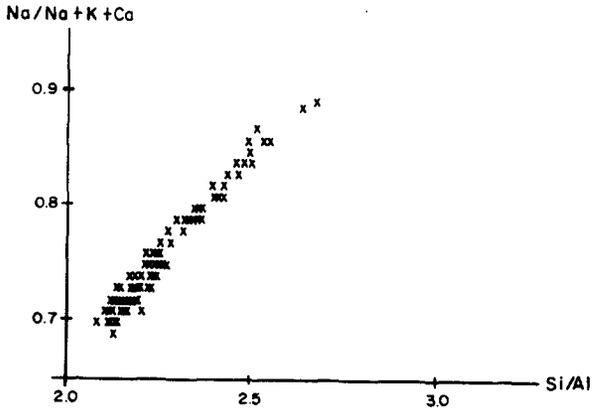

Fig. 12. Compositional variation in deformed plagioclase host grains (adjacent to segregation bands) and sub-grains and new grains of plagioclase in type IP aggregates.

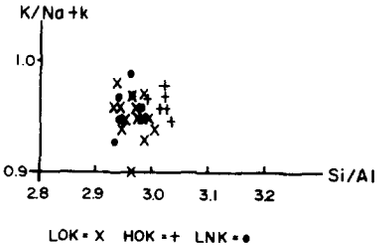

Fig. 13. Compositional variation in old K-feldspar grains at low (×) and high (+) bulk strains and in K-feldspar new grains (•) at low bulk strains; all for type IM aggregates.

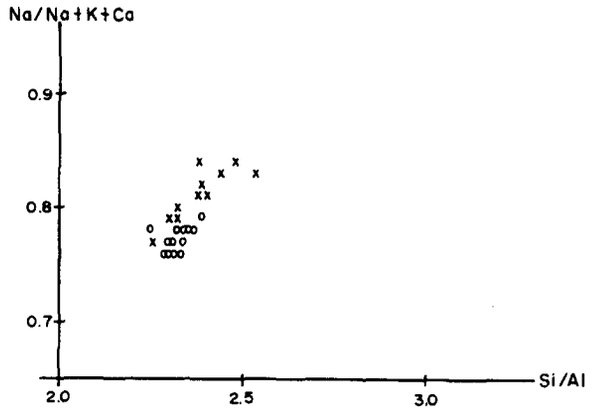

Fig. 14. Compositional variation in plagioclase new grains in type IM aggregates at low (crosses) and high (circles) bulk strains.

restricted and generally sodic in composition compared to plagioclase new grains derived from plagioclase parent grains. This reflects inheritance of a calcic component from the parent in the latter case. Plagioclase new grains derived from K-feldspar parents at higher bulk strains are more constant in composition than at low bulk strains. No systematic variation in plagioclase composition was detected across the type IM mantle aggregates.

The formation of segregation bands is approximately volume constant (Hanmer 1981b). Using the microprobe analyses, a simple constant volume mass balance equation can be derived (Gresens 1967).

$$100 \text{ plagioclase } (An_{28}) + 9.5\,Na_2O + 5.0\,SiO_2$$
$$\rightleftharpoons 99.98 \text{ plagioclase } (An_{10}) + 3.9\,CaO + 3.1\,Al_2O_3.$$

Obviously the source of the quartz core in the segregation bands was external to the host plagioclase grain.

Similarly, the microprobe analyses can be directly compared with the visible microstructure in the type IM recrystallized mantle aggregates. The 40 μm inner mantle plagioclase new grains, although now compositionally indistinguishable from the 10 μm new grains of the outer mantle, are sericitized. This, combined with the myrmekite growth at the mantle/core boundary, suggests that the inner mantle plagioclase was initially more calcic than at present. From the microprobe data, a more complete description of the K-feldspar/albite transformation with progressive strain is

(i) K-feldspar I
(ii) K-feldspar II 40 μm
(iii) oligoclase (An_{28}) 40 μm
(iv) albite (An_{10}) 10 μm.

From this sequence the association of 10 μm quartz drops with the coarser plagioclase, and their absence from finer aggregates, is explicable. Assuming constant volume, the mass balance equation for the K-feldspar → oligoclase reaction is

$$100 \text{ K-feldspar} + 8.74\,Na_2O + 4.8\,CaO + 4.9Al_2O_3$$
$$\rightleftharpoons 101.8 \text{ oligoclase} + 16.3\,K_2O + 2.1\,SiO_2$$

whereas the oligoclase → albite transformation consumes

proportionally twice as much quartz as produced by this reaction. Quartz is therefore initially evolved as interstitial grains. Localization of the quartz at plagioclase new grain boundaries and triple points suggests impurity segregation of SiO_2 by diffusion (Byerly & Vogel 1973). With progressively increasing strain the quartz drops are resorbed into the more sodic plagioclase. The balance of SiO_2 not furnished by drop resorption can be supplied by the quartz veins of the parent K-feldspar which are truncated at the core-mantle boundary.

DISCUSSION

Microstructure

The feldspars examined here contain an assemblage of microstructures (veins, fractures, kinks, segregation bands, recrystallized aggregates) which taken together represent a brittle–ductile transitional behaviour. Some of the veins however, are not brittle dilational structures. The segregation bands in plagioclase are not brittle fractures because: (a) The observed mineral modifications occur irrespective of band type and cannot be specifically related to the discontinuities of type (3) bands. Even these discontinuities, although suggestive of microfracturing, do not produce macroscopic cracks and therefore are not unequivocal brittle structures (Paterson 1978, p. 2). (b) The existence and persistence of rounded kink hinges within the bridges of type (2) bands is not associated with brittle failure. A minor component of dilation within the size range (25–100 μm) common to both incipient and mature bands cannot be excluded in the type (1) segregation bands. However, the persistence of rounded kink hinges and of discrete discontinuities within the bridges precludes dilation in bands of types (2) and (3). Indeed, the association of type (2) bands with kinking suggests that they are compressional rather than dilational structures.

Segregation bands are not crack–seal veins (Ramsay 1980) because: (a) Similarly oriented non-albitic kinks are present in the same specimens. (b) The quartz cores are often monocrystalline, never fibrous and lack 'inclusion bands' (Ramsay 1980). (c) Neither the quartz cores nor the twin-free incipient type (1) bands are in optical continuity with the well twinned host plagioclase. (d) The evolution from quartz beads to continuous quartz cores is not simply related to the segregation band width. Indeed the quartz appears to replace the sodic plagioclase of the segregation band. (e) The discontinuities in incipient type (3) bands are not "median inclusion surfaces" (Ramsay 1980), but continuous and discrete. (f) Types (2) and (3) segregation bands are non-dilational.

Furthermore, segregation bands are not simple subcritical stress corrosion cracks (Kerrich *et al.* 1980) since: (a) reaction zones in type (3) bands are adjacent to the discontinuity as opposed to within a crack; (b) stress corrosion crack fill is plagioclase of host composition and (c) there is no evidence for localization of reactions at crack tips.

Recrystallization

In the polycrystalline feldspar aggregates, some new grains of plagioclase are bent or kinked and show undulose extinction. The large substructural domains in K-feldspar type IIM aggregates contain still smaller K-feldspar subgrains. Furthermore, the small ($< 40\,\mu$m) sodic plagioclase new grains in type IM aggregates form by recrystallization of larger ($> 40\,\mu$m) K-feldspar new grains in regions of high strain (mantles, kinks, shears). The aggregates therefore constitute a dynamic recrystallization microstructure.

In plagioclase, type IP aggregates developed at sites of locally high strain concentrations resemble the subgrain associated microstructure described by Marshall & Wilson (1976) and Marshall & McLaren (1977a, 1977b).

In type IIP aggregates, subgrains and new grains are up to two orders of magnitude larger than those of type IP. This suggests formation by a different mechanism. The boundaries of the type IIP subgrains closely resemble the descriptions of subcritical corrosion cracks of Kerrich *et al.* (1980). The microstructural contrast between type IP and type IIP aggregates may reflect a greater influence of microcracking in the latter case. Since the effect of confining pressure is to homogenize the distribution of microcrack initiation (Paterson 1978, p. 156), this hypothesis could account for the distribution of the subgrains throughout the volume of the old grain. The grain size of the type IIP aggregates would therefore be confining pressure dependent.

Use of the term 'subgrain' in type IIP aggregates is somewhat ambiguous since it is not applied to substructural elements bounded by dislocation walls (e.g. White 1973, Nicolas & Poirier 1976, p. 47). The term 'fragment' however, suggests brittle cataclasis which is not warranted by the observations, and 'domain' is here applied to K-feldspar substructures influenced by pre-existing internal growth boundaries. The term 'subgrain' has therefore been used *sensu lato*.

In type IM aggregates, initial recrystallization apparently involves subgrain rotation, since the subgrains are less misoriented with respect to the host than are the new grains.

In type IIM aggregates, the irregular shaped substructural domains (Fig. 9b) closely resemble the growth domains illustrated by Willaime *et al.* (1979, fig. 1b) in an undeformed single sanidine crystal. They interpret the domain limits as growth boundaries. The more regular lozenge shaped substructural domains (Fig. 9a) are bounded by conjugate shears morphologically similar to the deformation lamellae produced by Willaime *et al.* (1979) by deformation of their single sanidine crystal. This suggests that the type IIM substructural domains may form by shear modification of pre-existing growth boundaries. Others are apparently crystallographically controlled. Formation of an aggregate by growth boundary slip would result in strain softening of the host grain and facilitate further deformation leading to the observed subgrain and new grain development within and along the boundaries of the substructural domains.

Subgrains are not observed to accompany the ultimate grain refinement in either type IM or type IIM aggregates. The finest grain size is however accompanied in both cases by a marked change in feldspar compositions (K-feldspar → oligoclase → albite). Whatever the mechanism(s) of recrystallization might be, the driving force may include a contribution from the negative change in free energy due to the change in chemical composition (e.g. Etheridge & Hobbs 1974, Poirier & Guillopé 1979, Allison *et al.* 1979, Kerrich *et al.* 1980).

Geochemistry

The microprobe data indicates the operation of mass transfer in both the segregation bands and the recrystallized aggregates. From the analyses, the sodic plagioclase composition of the initial segregation bands may be derived by the addition of Na_2O and SiO_2 to the host grain with concomitant loss of CaO and Al_2O_3. The subtracted components may now reside in accessory phases such as clinozoisite, but the source of the added components must lie outside of the host grain, i.e. in the grain boundary fluid. It is inferred, from the localized nature of the compositional modifications of the host grains, that the added components enter the segregation band by preferential, perhaps strain enhanced (White & Knipe 1978), diffusion along the bands. The hydrous nature of the accessory minerals suggests the presence of water, which itself would enhance diffusion.

The limited compositional variation within the sodic plagioclase new grains in type IM aggregates at high strains compared to that at low strains, given the constant composition of the K-feldspar parent grains in the different specimens examined, implies strain enhancement of diffusion. Kerrich *et al.* (1980) consider the presence of quartz grains in sodic plagioclase mantles on feldspar cores to result, at least in part, from mechanical incorporation and use it as a criterion for superplastic behaviour of the aggregate. The absence of quartz from the albite mantles of this study does not support their hypothesis. This study does however, provide further evidence in support of reaction enhanced ductility (White & Knipe 1978, Allison *et al.* 1979) in mantle aggregates.

Diffusion

Without TEM data, only the presence or absence of optically visible subgrains can be established. The presence of dislocations or submicroscopical cracks can however be conjectured from the presence of the subgrains and of undulatory extinction (White 1973, Sacerdoti *et al.* 1980). If such submicroscopic structures are present in the segregation bands and recrystallized aggregates, they could provide the key to understanding the observed compositional changes.

Diffusion in feldspars occurs by a vacancy mechanism (Petrovic 1974) and vacancy–interstitial ion pairs diffuse preferentially towards high energy surfaces such as high angle boundaries, dislocations and microcracks (Byerly & Vogel 1973, Knipe 1980). Concentrations of dislocations provide pathways of easy diffusion (White 1975). Na^+, K^+ exchange itself is known to produce local high stress concentrations and lead to enhanced microcracking (Petrovic & Skinner 1970, Barnett & Kerrich 1980). In other words, feedback may operate between strain enhanced diffusion and reaction enhanced ductility (White & Knipe 1978).

The replacement of K-feldspar by oligoclase and of oligoclase by albite imply the mass transfer of indeterminate quantities of alkalis, Al^{3+}, Ca^{2+}, Si^{4+}, etc. Whereas some of the liberated K^+ may now reside in the interstitial biotites of the type IP and IM aggregates and in K-feldspar grains in pressure shadows on plagioclase porphyroclasts, these new phases are unlikely to account for the volume of original K-feldspar which has been replaced. Furthermore, the source for the additional Na^+ required for the oligoclase → albite reaction is not self evident. The suite of granites from which the samples for the present study were taken show a wide range of chemical composition, even within individual plutons (Strong *et al.* 1974, Strong & Dickson 1978). It has therefore not been feasible to examine the bulk chemical aspects of the whole rocks with progressive strain and the problem posed by the large scale transfer of alkalis, etc. remains.

CONCLUSIONS

Feldspars in granites deformed at moderate to elevated temperatures in the Northeast Newfoundland Shear Zone exhibit brittle–ductile transitional behaviour. The brittle or cataclastic component however, is markedly subordinate to the ductile component. Interaction of metamorphic (diffusion, reaction) and structural processes strain) plays a major role in the development of the microstructure through strain enhanced diffusion and reaction enhanced ductility.

(1) Some quartz-filled intragranular veins in K-feldspar are unequivocally brittle dilational fractures. However, some intragranular quartz-filled veins in plagioclase are ductile, non-dilational segregation bands formed by diffusion associated with kinking and microcracking.

(2) Two major types of polycrystalline aggregate form by dynamic recrystallization of plagioclase and K-feldspar. (a) IP and IM aggregates form core and mantle structures by normal subgrain associated recrystallization. (b) IIP aggregates form mortar structures by the rotation of very large subgrains (*s.l.*) between microcracks. The initial aggregate grain size is pressure dependent. IIM aggregates form a coarse domainal substructure by slip modification of pre-existing internal growth boundaries or by crystallographically controlled microshearing. Normal subgrain development within and along the domain boundaries produces a mortar structure.

(3) Grain size reduction below about 50 μm is accompanied by transformation of plagioclase (An_{28}) and K-feldspar to albite. The compositional variation of the plagioclase new grains decreases with increasing bulk strain of the rock.

Acknowledgements—Thanks to R. M. Mackay for invaluable assistance on the microprobe and to A. E. Aksu for equal assistance with the computing. Special thanks to T. J. Calon for discussion and critical review of an earlier draft of the manuscript. Thanks to Dalhousie Geology Department for hospitality, facilities and encouragement throughout the course of this work, especially to P. E. Schenk for photographic facilities. A Killam Post-Doctoral Fellowship is most gratefully acknowledged.

REFERENCES

Allison, I., Barnett, R. L. & Kerrich, R. 1979. Superplastic changes in crystal chemistry of feldspars. *Tectonophysics* **53**, T41–T46.

Barnett, R. L. & Kerrich, R. 1980. Stress corrosion cracking in biotite and feldspar. *Nature, Lond.* **283**, 185–187.

Beach, A. 1975. The geometry of en-echelon vein arrays. *Tectonophysics* **28**, 245–263.

Berthé, D., Choukroune, P. & Jegouzo, P. 1979a. Orthogneiss mylonite, and non-coaxial deformation of granites: the example of the South Armorican Shear Zone. *J. Struct. Geol.* **1**, 31–42.

Berthé, D., Choukroune, P. & Gapais, D. 1979b. Orientations préférentielles du quartz et orthognessification progressive en regime cisaillant: l'éxemple due cisaillement sud armoricain. *Bull. Mineral.* **102**, 265–272.

Blackwood, R. F. 1977. Geology of the East Half of the Gambo (2D/16) map area and the Northwest Portion of the St. Brendans (2C/16) map area, Newfoundland. *Newfoundland Department of Mines and Energy, Min. Dev. Div., Report* **77–5**, 20pp.

Borg, I. Y. & Heard, N. H. 1970. Experimental deformation of plagioclase. In: *Experimental and Natural Rock Deformation* (edited by Paulitsch P.), Springer, Berlin, 375–403.

Burg, J. P. & Laurent, P. 1978. Strain analysis of a shear zone in a granodiorite. *Tectonophysics* **47**, 15–42.

Byerly, G. R. & Vogel, T. A. 1973. Grain boundary processes and development of metamorphic plagioclase. *Lithos* **6**, 183–202.

Carter, N. L. 1971. Static deformation of silica and silicates. *J. geophys. Res.* **76**.

Carter, N. L. 1976. Steady state flow of rocks. *Rev. Geophys. Space Phys.* **14**, 201–360.

Debat, P., Siriey, S., Deramond, J. & Soula, J. C. 1975. Paléodéformations d'un massif orthognessisque (Massif des Cammazes, Montagne Noire Occidentale, France). *Tectonophysics* **28**, 159–183.

Debat, P., Soula, J. C., Kubin, L. & Vidal, J. L. 1978. Optical studies of natural deformation microstructures in feldspars (gneiss and pegmatites from Occitania, Southern France). *Lithos* **9**, 132–145.

Deer, W. A., Howie, R. A. & Zussman, J. 1966. *An Introduction to the Rock Forming Minerals*. Longman.

Etheridge, M. A. & Hobbs, B. E. 1974. Chemical and deformational controls on the recrystallization of micas. *Contr. Miner. Petrol.* **43**, 111–124.

Eisbacher, G. H. 1970. Deformation of mylonitic rocks and fractured granites in Cobequid Mountains, NS, Canada. *Bull. geol. Soc. Am.* **81**, 2009–2020.

Gresens, R. L. 1967. Composition—volume relationships of metasomatism *Chem. Geol.* **2**, 47–65.

Hanmer, S. K. 1980. Major Acadian sinistral shear in Newfoundland: geological support for paleomagnetic models. *Geol. Ass. Can. Joint Ann. Meet. Programme with abstracts*, **5**, 58.

Hanmer, S. K. 1981a. Tectonic significance of the Northeastern Gander Zone, Newfoundland: an Acadian ductile shear zone. *Can. J. Earth. Sci.* **18**, 120–135.

Hanmer, S. K. 1981b Segregation bands in plagioclase: non-dilational en-echelon quartz veins formed by strain enhanced diffusion *Tectonophysics* **79**, T53–T61.

Jayasinghe, N. R. 1978. Geology of the Wesleyville Map Area (2F/4) and Musgrave Harbour East (2F/5) Map Areas, Newfoundland. *Newfoundland Depart. Mines and Energy, Min. Dev. Div., Report* **78–18**, 11pp.

Kent, D. V. & Opdyke, N. D. 1978. Paleomagnetism of the Devonian Catskill Red Beds: Evidence for motion of the coastal New England–Canadian Maritimes Region relative to cratonic North America. *J. geophys. Res.* **83**, 4441–4450.

Kerrich, R., Allison, I., Barnett, R. L., Moss, S. & Starkey, J. 1980. Microstructural and chemical transformation accompanying deformation of granite in a shear zone at Mieville, Switzerland: with implications for stress corrosion cracking and superplastic flow. *Contr. Miner. Petrol.* **73**, 221–242.

Knipe, R. J. 1980. Distribution of impurities in deformed quartz and its implications for deformation studies. *Tectonophysics* **64**, T11–T18.

Knipe, R. J. & White, S. 1979. Deformation in low grade shear zones in the Old Red Sandstones, S. Wales. *J. Struct. Geol.* **1**, 53–66.

Lally, J. S., Fisher, R. M., Christie, J. M., Griggs, D. T., Heuer, A. H., Nord, G. L. & Radcliffe, S. V. 1972. Electron petrography of Apollo 14 and 15 samples. *Lunar Sci. Conf. Houston, Lunar Sci. Inst. Contrib. 3rd* **88**, 469–471.

Lister, G. S. & Paterson, M. S. 1979. The simulation of fabric development during deformation and its application to quartzite: fabric transitions. *J. Struct. Geol.* **1**, 99–1115.

Lister, G. S. & Price, G. P. 1978. Fabric development in a quartz-feldspar mylonite. *Tectonophysics* **49**, 37–78.

Lorimer, G. W., Nissen, H. U. & Champness, P. E. 1974. High voltage electron microscopy of deformed sodic plagioclase from an Alpine gneiss. *Schweiz. miner. petrogr. Mitt.* **54**, 707–715.

Marshall, D. B. & McLaren, A. C. 1977a. The direct observation and analysis of dislocations in experimentally deformed plagioclase feldspars. *J. Mater. Sci.* **12**, 843–903.

Marshall, D. B. & McLaren, A. C. 1977b. Deformation mechanisms in experimentally deformed plagioclase feldspars. *Phys. Chem. Miner.* **1**, 315–370.

Marshall, D. B., Vernon, R. H. & Hobbs, B. E. 1976. Experimental deformation and recrystallization of a peristerite. *Contr. Miner. Petrol.* **57**, 49–54.

Marshall, D. B. & Wilson, C. J. L. 1976. Recrystallization and peristerite formation in albite. *Contr. Miner. Petrol.* **57**, 55–69.

Morris, W. A. 1976. Transcurrent motion determined paleomagnetically in the Northern Appalachians and Caledonides and the Acadian Orogeny. *Can. J. Earth Sci.* **13**, 1236–1243.

Nicholas, A. and Poirier, J. P. 1976. *Crystalline Plasticity and Solid State Flow in Metamorphic Rocks*. Wiley, New York.

Paterson, M. S. 1978. *Experimental Rock Deformation: The Brittle Field*. Springer, Berlin, 254.

Petrovic, R. 1974. Diffusion of alkali ions in alkali feldspar. In: *The Feldspars*. (edited by Mackenzie, W. S. & Zussman, J.). Proc. NATO Adv. Study Instit., Manchester Univ. Press, 174–182.

Petrovic, R. & Skinner, B. J. 1970. Deformation of alkali feldspars as a consequence of alkali diffusion, *Eos Trans. Am. geophys. Un.* **51**, 439.

Poirier, J. P. & Guillopé, M. 1979. Deformation induced recrystallization of minerals. *Bull. Mineral.* **102**, 67–74.

Ramsay, J. G. 1980. The crack-seal mechanism of rock deformation. *Nature, Lond.* **284**, 135–139.

Ramsay, J. G. & Graham, R. H. 1970. Strain variation in shear belts. *Can. J. Earth Sci.* **7**, 786–813.

Sacerdoti, M., Labernardiere, H. & Gandais, M. 1980. Transmission electron microscope (T.E.M.) study of geologically deformed potassic feldspars. *Bull. Mineral.* **103**, 148–155.

Seifert, K. E. 1965. Deformation bands in albite. *Am. Miner.* **50**, 1469–1472.

Stesky, R. M. 1977. Mechanisms of high temperature frictional sliding in Westerly granite. *Can. J. Earth Sci.* **15**, 361–375.

Strong, D. F., Dickson, W. L., O'Driscoll, C. F., Kean, B. F. 1974. Geochemistry of Eastern Newfoundland granitoid rocks. *Newfoundland Department of Mines and Energy, Min. Dev. Div., Report* **74–3**: 140.

Strong, D. F. & Dickson, W. L. 1978. Geochemistry of Paleozoic granitoid plutons from contrasting tectonic zones of N.E. Newfoundland. *Can. J. Earth Sci.* **15**, 145–156.

Sturt, B. A. 1969. Wrench faulting deformation and annealing recrystallization during almandine–amphibolite facies regional metamorphism. *J. Geol.* **77**, 319–332.

Sylvester, A. G., Oertel, G., Nelson, C. A. & Christie, J. M. 1978. Papoose Flat pluton: a granitic blister in the Inyo Mnts., California. *Bull. geol. Soc. Am.* **89**, 1205–1219.

Talbot, C. J. 1979. Fold trains in a glacier of salt in southern Iran. *J. Struct. Geol.* **1**, 5–18.

Tullis, J. & Yund, R. A. 1977. Experimental deformation of dry Westerly granite. *J. geophys. Res.* **82**, 5705–5718.

Tullis, J. & Yund, R. A. 1980. Hydrolytic weakening of experimentally deformed Westerly granite and Hale albite rock. *J. Struct. Geol.* **2**, 439–451.

Tullis, J., Shelton, G. L. & Yund, R. A. 1979. Pressure dependence of rock strength: implications for hydrolytic weakening. *Bull. Mineral.* **102**, No. 114.

Van Der Voo, R., French, A. N. & French, R. B. 1979. A paleomagnetic pole position from the folded Upper Devonian Catskill Red Beds and its tectonic implications. *Geology* **7**, 345–348.

Vernon, R. H. 1975. Natural deformation and recrystallization of a plagioclase grain. *Am. Miner.* **60**, 884–888.

Vidal, J. L., Kubin, L., Debat, P. & Soula, J. C. 1980. Deformation and dynamic recrystallization of K-feldspar augen in orthogneiss from Montagne Noire, Occitania, Southern France. *Lithos* **13**, 247–255.

Wakefield, J., 1977. Mylonitization in the Lethakane Shear Zone, E. Botswana *J. geol. Soc. Lond.* **133**, 263–275.

White, S. 1973. The dislocation structures responsible for the optical effects in some naturally deformed quartz. *J. Mater. Sci.* **8**, 490–499.

White, S. 1975. Tectonic deformation and recrystallization of plagioclase. *Contr. Miner. Petrol.* **50**, 287–304.

White, S. 1976. The effects of strain on the microstructures, fabrics and deformation mechanisms in quartzite. *Phil. Trans. R. Soc.* **A283**, 69–86.

White, S., Burrows, S. E., Carreras, J., Shaw, N. D. & Humphreys, P. J. 1980. On mylonites in ductile shear zones. *J. Struct. Geol.* **2**, 175–188.

White, S. & Knipe, R. J. 1978. Transformation and reaction enhanced ductility in rocks. *J. geol. Soc. Lond.* **135**, 513–516.

Willaime, C. & Gandais, M. 1977. Electron microscope study of plastic defects in experimentally deformed alkali feldspars. *Bull. Soc. fr. Minér. Cristallogr.* **100**, 263–271.

Willaime, C., Christie, J. M. & Kovacs, M. P. 1979. Experimental deformation of K-feldspar single crystals. *Bull. Mineral.* **102**, 168–177.

Williams, H. 1979. The Appalachian orogen in Canada. *Can. J. Earth Sci.* **16**, 792–807.